



**HAL**  
open science

## **A genome-wide association and prediction study in grapevine deciphers the genetic architecture of multiple traits and identifies genes under many new QTLs**

Timothée Flutre, Loïc Le Cunff, Agota Fodor, Amandine Launay, Charles Romieu, Gilles Berger, Yves Bertrand, Nancy Terrier, Isabelle Beccavin, Virginie Bouckenoghe, et al.

### ► To cite this version:

Timothée Flutre, Loïc Le Cunff, Agota Fodor, Amandine Launay, Charles Romieu, et al.. A genome-wide association and prediction study in grapevine deciphers the genetic architecture of multiple traits and identifies genes under many new QTLs. *G3*, 2022, 10.1093/g3journal/jkac103 . hal-03697272

**HAL Id: hal-03697272**

**<https://hal.inrae.fr/hal-03697272>**

Submitted on 16 Jun 2022

**HAL** is a multi-disciplinary open access archive for the deposit and dissemination of scientific research documents, whether they are published or not. The documents may come from teaching and research institutions in France or abroad, or from public or private research centers.

L'archive ouverte pluridisciplinaire **HAL**, est destinée au dépôt et à la diffusion de documents scientifiques de niveau recherche, publiés ou non, émanant des établissements d'enseignement et de recherche français ou étrangers, des laboratoires publics ou privés.



Distributed under a Creative Commons Attribution 4.0 International License

# A genome-wide association and prediction study in grapevine deciphers the genetic architecture of multiple traits and identifies genes under many new QTLs

Timothée Flutre <sup>1,2,3</sup>, Loïc Le Cunff <sup>2,4</sup>, Agota Fodor,<sup>1,2</sup> Amandine Launay <sup>1,2</sup>, Charles Romieu <sup>1,2</sup>, Gilles Berger,<sup>1,2</sup> Yves Bertrand,<sup>1,2</sup> Nancy Terrier,<sup>1</sup> Isabelle Beccavin,<sup>4</sup> Virginie Bouckennooghe,<sup>2,4</sup> Maryline Roques,<sup>2,4</sup> Lucie Pinasseau,<sup>5</sup> Arnaud Verbaere,<sup>5</sup> Nicolas Sommerer,<sup>5</sup> Véronique Cheynier <sup>5</sup>, Roberto Bacilieri <sup>1,2</sup>, Jean-Michel Boursiquot,<sup>1,2</sup> Thierry Lacombe <sup>1,2</sup>, Valérie Laucou,<sup>1,2</sup> Patrice This <sup>1,2</sup>, Jean-Pierre Péros <sup>1,2</sup> and Agnès Doligez <sup>1,2</sup>

<sup>1</sup>AGAP Institut, Univ Montpellier, CIRAD, INRAE, Institut Agro, 34398 Montpellier, France

<sup>2</sup>UMT Géno-Vigne, 34398 Montpellier, France

<sup>3</sup>Université Paris-Saclay, INRAE, CNRS, AgroParisTech, GQE—Le Moulon, 91190 Gif-sur-Yvette, France

<sup>4</sup>IFV, 30240 Le Grau-du-Roi, France

<sup>5</sup>SPO, Univ Montpellier, INRAE, Institut Agro, 34060 Montpellier, France

\*Corresponding author: AGAP Institut, Univ Montpellier, CIRAD, INRAE, Institut Agro, 34398 Montpellier, France. Email: timothee.flutre@inrae.fr; \*Corresponding author: AGAP Institut, Univ Montpellier, CIRAD, INRAE, Institut Agro, 34398 Montpellier, France. Email: agnes.doligez@inrae.fr

## Abstract

To cope with the challenges facing agriculture, speeding-up breeding programs is a worthy endeavor, especially for perennial species such as grapevine, but requires understanding the genetic architecture of target traits. To go beyond the mapping of quantitative trait loci in bi-parental crosses, we exploited a diversity panel of 279 *Vitis vinifera* L. cultivars planted in 5 blocks in the vineyard. This panel was phenotyped over several years for 127 traits including yield components, organic acids, aroma precursors, polyphenols, and a water stress indicator. The panel was genotyped for 63k single nucleotide polymorphisms by combining an 18K microarray and genotyping-by-sequencing. The experimental design allowed to reliably assess the genotypic values for most traits. Marker densification via genotyping-by-sequencing markedly increased the proportion of genetic variance explained by single nucleotide polymorphisms, and 2 multi-single nucleotide polymorphism models identified quantitative trait loci not found by a single nucleotide polymorphism-by-single nucleotide polymorphism model. Overall, 489 reliable quantitative trait loci were detected for 41% more response variables than by a single nucleotide polymorphism-by-single nucleotide polymorphism model with microarray-only single nucleotide polymorphisms, many new ones compared with the results from bi-parental crosses. A prediction accuracy higher than 0.42 was obtained for 50% of the response variables. Our overall approach as well as quantitative trait locus and prediction results provide insights into the genetic architecture of target traits. New candidate genes and the application into breeding are discussed.

**Keywords:** GWAS; genomic prediction; grapevine; *Vitis vinifera* L; genotyping-by-sequencing; yield components; secondary metabolites; genetic architecture; candidate genes

## Introduction

With the 2 major challenges facing perennial fruit crops in general and grapevine in particular, i.e. decreasing phytosanitary products such as fungicide treatments and adapting to climate change, harnessing existing genetic diversity (Wolkovich et al. 2018) and breeding new varieties (Adam-Blondon et al. 2011) are both important levers. For the latter, many studies aimed at deciphering the genetic architecture of traits of interest by mapping quantitative trait loci (QTLs) in bi-parental progenies (Vezzulli et al. 2019). However, this approach suffers from several drawbacks: the limited allelic diversity in parents, the low number of recombination events in the progeny, the upward bias of estimated QTL effects, and the underestimation of the polygenic contribution for prediction purposes (Cardon and Bell 2001). As a result, all traits currently involved

in grapevine marker-assisted selection (Vezzulli et al. 2019) are controlled by major genes, such as resistance to downy and powdery mildews (Di Gaspero et al. 2007), black rot (Rex et al. 2014), sex (Picq et al. 2014), berry color (Fournier-Level et al. 2009), seedlessness (Mejía et al. 2011), and Muscat aroma (Duchêne et al. 2009).

To overcome these limits, a few genome-wide association studies (GWASs) have been performed in cultivated grapevine diversity panels but, due to various reasons, failed to identify many new QTLs. Several articles (Myles et al. 2011; Zarouri 2016; Migicovsky et al. 2017; Laucou et al. 2018) harnessed phenotypic data from genetic resources repositories collected without a proper experimental design. Moreover, the first 3 articles cited used at most 10k SNPs despite the low extent of linkage disequilibrium (LD) (Myles et al. 2011; Nicolas et al. 2016). Among other

Received: January 21, 2022. Accepted: April 21, 2022

© The Author(s) 2022. Published by Oxford University Press on behalf of Genetics Society of America.

This is an Open Access article distributed under the terms of the Creative Commons Attribution License (<https://creativecommons.org/licenses/by/4.0/>), which permits unrestricted reuse, distribution, and reproduction in any medium, provided the original work is properly cited.

articles, Zhang *et al.* (2017) focused on a single binary trait with a major QTL, seedlessness; Yang *et al.* (2017) used only 187 SSRs and 96 genotypes; Sargolzaei *et al.* (2020) focused on disease resistance using an 18K SNP microarray; Naegele *et al.* (2021) used at most 14k SNPs obtained by sequencing.

Moreover, most of these articles as well as one using 32k SNPs obtained with sequencing (Guo *et al.* 2019) used only SNP-by-SNP models. However, multi-SNP models have the advantage of explicitly assuming a genetic architecture, be it sparse with few major QTLs or dense with many small-effect QTLs, allowing them to benefit from a potential gain in power (Zhang *et al.* 2019). Furthermore, the effects of QTLs are often overestimated (Xu 2003) which leads to poor prediction (Meuwissen *et al.* 2001). Multi-SNP models provide a straightforward way to efficiently perform genomic prediction (de los Campos *et al.* 2013), notably for traits devoid of major QTLs.

Consequently, our objective was to perform whole-genome association and prediction for various traits of interest in grapevine breeding, likely to display different genetic architectures. We aimed at finding out to what extent genetic variation contributes to phenotypic variation, how it is organized in sparse and dense genetic components, how accurate genomic prediction might be, and which genes are present under the QTLs uncovered. Our approach builds on a large diversity panel of 279 *Vitis vinifera* L. cultivars (Nicolas *et al.* 2016) defined from the French collection of grapevine genetic resources and overgrafted in the vineyard in 5 randomized complete blocks. The panel was phenotyped over several years and under different conditions for 127 traits, including yield components, organic acids, aroma precursors, polyphenols, and a water stress indicator, which, along with 25 derived variables, totaled 152 response variables. The cultivars were genotyped with both microarray and sequencing after a reduction of genomic complexity (genotyping-by-sequencing, GBS), reaching a total of 63k SNPs. QTL detection and genomic prediction were then performed with multi-SNP models assuming different genetic architectures, and positional candidate genes were searched for under QTLs.

## Materials and methods

### Plant material and field trial

The panel of 279 cultivars of *Vitis vinifera* L. was designed to limit relatedness (any pair of cultivars in the panel corresponds to distinct genotypes with no parent in common) and is weakly structured in 3 genetic groups (Nicolas *et al.* 2016). In 2009, at the Domaine du Chapitre of Institut Agro Montpellier (Villeneuve-lès-Maguelone, France), the 279 cultivars as well as a control (cv. Marselan) were all overgrafted onto 6-year-old Marselan vines, itself grafted on rootstock Fercal, in a complete randomized block design with 5 blocks (A to E, Supplementary Fig. 1). Because of failed overgrafting, precocious death or fertility issues, only 270 cultivars out of the 279 in the whole panel could be phenotyped. The density of the field trial was 3,300 plants/ha (1 m between plants along the same rank and 2.5 m between ranks). Each of the 5 blocks contained 1 plant of each panel cultivar as well as a regular mesh of over-grafts of Marselan as control (between 23 and 39 per block). The double-cordon training system was applied.

A random subset of 21 full-sib genotypes of a Syrah × Grenache progeny, together with the 2 parents, was also used to assess out-of-sample genomic prediction. The field design had 2 random complete blocks established in 2003 as already described (Doligez *et al.* 2013). Each block contained the whole progeny (191 offsprings, one subplot each) as well as both parents (9 subplots each). Each subplot contained 5 grafted plants of the same genotype.

## Phenotyping

Here, we will use the term “trait” for any plant feature for which raw data were collected, whatever the year and condition. However, in our analyzes we use the term “response variable” because: (1) for some traits, data were acquired in different years and conditions, and hence analyzed separately; (2) we also combined several traits to define new variables. In the end, we thus analyzed 152 response variables from 127 traits.

In 2011 and 2012, the trial was not irrigated, and all the plants of the panel cultivars and controls were concurrently phenotyped. For each plant, we recorded the number of clusters (NCBLU) and harvested 3 clusters at 20°Brix, which provided the sampling date (SAMPLDAY, in days since January 1). We recorded mean cluster weight (MCW, in g), mean cluster length (in cm), mean cluster width (in cm), and cluster compactness (from 1 to 9 on the OIV 204 scale; OIV, 2009). One hundred berries randomly sampled from the central third of clusters were weighed, providing the mean berry weight (MBW, in g). In the winters of 2011–2012 and 2012–2013, the number of woody shoots (NBWS) and pruning weight (PRUW, in kg) were recorded for each plant. In 2011, the veraison date (onset of ripening, VER, in days since January 1) was also recorded. Two variables were computed from these traits: the veraison-maturity interval (VERMATU as SAMPLDAY—VER, in days), and plant vigor (VIG as PRUW/NBWS, in kg). In 2011 and 2012, juices were made from the sampled berries and analyzed to measure  $\delta^{13}\text{C}$  (D13C) as previously detailed (Pinasseau, Vallverdú-Queralt, *et al.* 2017). In 2012 were also determined glucose (GLU), fructose (FRU), malate (MAL), tartrate (TAR), shikimate (SHI), and citrate (CIT) concentrations, all in  $\mu\text{Eq l}^{-1}$ , as previously described (Rienth *et al.* 2016). Six variables were computed from these traits: the sum of glucose and fructose (GLUFRU), glucose divided by fructose (GLUONFRU), malate divided by either tartrate (MALTAR), shikimate (SHIKTAR), or citrate (CITAR) and the sum of glucose and fructose (GLUFRUTAR).

In 2014 and 2015, irrigation was applied to blocks C, D, and E only (Pinasseau, Vallverdú-Queralt, *et al.* 2017), and only panel cultivars were phenotyped. As above, 3 clusters per plant were harvested at 20°Brix, providing the MCW (in g). Berries sampled from different blocks with the same water treatment were pooled per cultivar. More details on berry sampling and processing, as well as polyphenols and  $\delta^{13}\text{C}$  measurements and analysis are described elsewhere (Pinasseau, Vallverdú-Queralt, *et al.* 2017). From the data available on the 105 different polyphenols in  $\mu\text{g}$  per berry (Pinasseau, Verbaere, *et al.* 2017), a few typos were corrected and 17 extra variables were calculated (Pinasseau, Vallverdú-Queralt, *et al.* 2017). In addition, 2 aroma precursors,  $\beta$ -damascenone (BDAM, in  $\mu\text{g l}^{-1}$ ) (Kotseridis *et al.* 1999) and potential dimethyl sulfide (PDMS, in  $\mu\text{g l}^{-1}$ ) (Segurel *et al.* 2005) were also quantified. The volume and weight of juice samples were recorded, allowing to assess their effects when included as cofactors in the statistical analyses.

A total of 127 traits were phenotyped, from which 25 extra variables were computed. Because irrigation was applied to some blocks only in 2014–2015, the few traits phenotyped both in 2011–2012 and in 2014–2015 were analyzed separately. Overall, 152 response variables were analyzed (Supplementary Tables 1 and 2).

The sanitary status of cultivars regarding the presence of 5 viruses (CNa, GLRaV1, GLRaV2, GLRaV3, and GFkV) was assessed by ELISA from plants at INRAE Vassal (Marseillan, France). Flower sex (OIV 151) and berry skin color (OIV 225) of each panel cultivar were retrieved from (Laucou *et al.* 2018) and completed

with the database of INRAE Vassal germplasm repository ([https://bioweb.supagro.inra.fr/collections\\_vigne/Home.php?l=EN](https://bioweb.supagro.inra.fr/collections_vigne/Home.php?l=EN)).

Berry weight was phenotyped on the Syrah × Grenache cross in 2005, 2006, and 2007 in the same way as on the panel (Doligez et al. 2013), except that 8 clusters per genotype and per block were harvested instead of 3.

## Genotyping

### Data acquisition and analysis of microarray SNPs

The panel and Syrah × Grenache progeny were genotyped with the GrapeReSeq 18k Vitis Illumina microarray (Laucou et al. 2018). Data processing (see Supplementary Text 1, Supplementary Figs. 2, 3, and Supplementary Table 2) resulted in 13,925 SNPs for 277 cultivars. After filtering on LD above 0.9 and minor allele frequency (MAF) below 0.05, 10,530 SNPs remained (see Supplementary Fig. 4), thereafter referred to as the “microarray-only” SNPs.

### Data acquisition and analysis of sequencing SNPs

The panel was also genotyped by sequencing (GBS, Elshire et al. 2011). Keygene NV owns patents and patent applications protecting its Sequence Based Genotyping technologies. Data processing consisted in read checking with FastQC version 0.1.2 (Andrews 2016), demultiplexing with a custom script, cleaning, and trimming with CutAdapt version 1.8.1 (Martin 2011), alignment on the PN40024 12Xv2 reference sequence (Canaguier et al. 2017) with BWA MEM version 0.7.12-r1039 (Li 2013) and realignment with GATK version 3.7 (DePristo et al. 2011), followed by variant and SNP calling with GATK HaplotypeCaller, and a final filtering step, notably to discard SNP genotypes with <10 reads or quality below 20 (see Supplementary Text 2 and Supplementary Table 3). It resulted in 184,145 SNPs with <30% missing data for the 279 panel cultivars.

### Joint imputation of microarray and GBS SNPs

The 13,925 microarray SNPs and 184,145 GBS SNPs for 277 common cultivars were combined into a set of 197,885 common SNPs (after duplicate removal) using coordinates on the 12Xv2 reference sequence (Canaguier et al. 2017). Missing data were imputed using LD with Beagle version 4.1-r862 (Browning and Browning 2009) as advised by Swarts et al. (2014) with window = 1,000, overlap = 450, ne = 10,000, and otherwise default parameters. After filtering for LD above 0.9, 90,007 SNPs remained (see Supplementary Fig. 3), and while subsequent filtering for MAF below 0.05 resulted in 63,105 SNPs (see Supplementary Fig. 4), thereafter referred to as the “microarray-GBS” SNPs. We also imputed the Syrah × Grenache SNP genotypes similarly using Beagle.

## Statistical modeling of phenotypic data

We performed a 2-stage analysis of each response variable using univariate regression models. In the first stage, estimates of total genotypic values were obtained (detailed in this section). In the second stage (see next section), these were regressed on SNP genotypes to identify QTLs, estimate their allelic effects and assess prediction accuracy.

To decrease the influence of potential outliers, all polyphenols (the compounds as well as the calculated variables) had their raw data automatically transformed with the natural log. For the other traits, when their raw phenotypic data were too skewed as visually assessed, they were also log-transformed (see Supplementary Fig. 5 and Supplementary Table 4).

### Assessment of spatial heterogeneity

In 2011–2012, phenotypic data for the control were spatially analyzed (Cressie 1993) in a way similar to Hamann et al. (2002).

First, a global linear model was fitted with R/stats with fixed effects for block, year, block-year interaction, PRUW, NBWS, vigor, and all 5 viruses (PRUW and vigor were discarded when vigor itself was the response). Facilitated by R/MuMIn version 1.40 (Bartoń 2017), model comparison was performed by maximum likelihood (ML), the best model being selected based on the corrected Akaike information criterion, AICc (Burnham and Anderson 2004). For each year separately, the empirical variogram of residuals from the best model was computed, on which several variogram models were fitted by ML with R/gstat version 1.1.5 (Pebesma 2004): exponential, spherical, gaussian, and Stein’s parametrization of the Matérn model. The variogram model with the smallest sum of squared errors was then used to perform spatial interpolation by kriging, i.e. best linear unbiased prediction (BLUP) of the control’s response variable at all locations. By visually assessing the slope of the best variogram model fitted to the empirical variogram (Supplementary Fig. 6) and the prediction errors from cross-validation (data not shown), it was concluded that there was no need to correct for spatial heterogeneity.

In 2014–2015, the control was not phenotyped, an irrigation treatment was applied, and samples from different blocks with the same irrigation level were pooled (Pinasseau, Vallverdú-Queralt, et al. 2017), hence preventing the assessment of any potential spatial heterogeneity as above.

### Estimation of genotypic values

For each response variable, a global linear mixed model was defined with multiple fixed effects [for the 2011–2012 data set: block, year, block-year interaction, PRUW, NBWS, vigor, and all 5 viruses, PRUW and vigor being discarded when vigor itself was the response; for the 2014–2015 data set: irrigation, year, irrigation-year interaction, °Brix (as there can be small deviations from 20°Brix)], and all 5 viruses, as well as the volume and weight of juice samples for BDAM and PDMS) together with 2 random effects (genotype and genotype-year interaction). The global model was fitted by ML with R/lme4 version 1.1.19 (Bates et al. 2015). The output was given to R/lmerTest version 3.1-2 (Kuznetsova et al. 2017) to use its function “step.” Backward elimination of random-effect terms was performed using likelihood ratio test, followed by backward elimination of fixed-effect terms using F-test for all marginal terms, i.e. terms that can be dropped from the model while respecting the hierarchy of terms in the model, with a 0.05 P-value threshold for both types of terms. The final model after backward elimination was then refitted by restricted ML (ReML) to obtain unbiased estimates of variance components and empirical BLUPs of genotypic values. The acceptability of underlying assumptions (homoscedasticity, normality, independence) was visually assessed by plotting residuals and BLUPs. Broad-sense heritability on a genotype-mean basis ( $H^2$ ) was computed using 2 estimators. The first assumes a balanced design (Falconer and Mackay 2009):  $H^2_C = \sigma_g^2 / [\sigma_g^2 + (\sigma_{gy}^2/n_y) + (\sigma_e^2/(n_y \times n_r))]$  where  $\sigma_g^2$  is the variance of the genotypic values,  $\sigma_{gy}^2$  is the variance of the genotype-year interactions,  $n_y$  is the arithmetic mean number of trials (years),  $\sigma_e^2$  is the variance of the errors (residuals), and  $n_r$  the arithmetic mean number of replicates per trial. The second estimator,  $H^2_U$ , allows for unbalanced data (see Oakey et al. 2006, for details). Robust confidence intervals for variance components, heritability and genotypic coefficient of variation were obtained by parametric bootstrap as recommended by Schweiger et al. (2016), using the percentile method (Carpenter and Bithell 2000) in the R/lme4 and R/boot packages. In the Syrah × Grenache progeny, empirical BLUPs of genotypic values for berry weight were obtained in the same way.

## Statistical modeling of genotypic data

### Genetic architecture assumed sparse

We used 2 types of models to perform genome-wide association testing and detect QTLs. The first is the SNP-by-SNP model as implemented in GEMMA version 0.97 (Zhou and Stephens 2012). For each SNP  $p$ ,  $eBLUP(\mathbf{g}) = \mathbf{1}\mu + M_{a,p}\beta_p + \mathbf{u} + \mathbf{e}$  where  $eBLUP(\mathbf{g})$  is a vector of responses of length  $N$ ,  $M_{a,p}$  is a vector of length  $N$  with the genotypes at the  $p$ th SNP (additive coding),  $\beta_p$  is its effect modeled as fixed,  $\mathbf{u} \sim N_N(\mathbf{0}, \sigma_u^2 A)$  is a vector of length  $N$  corresponding to a polygenic effect modeled as random where the covariance matrix  $A$  contains additive genetic relationships (Vitezica et al. 2013), and  $\mathbf{e} \sim N_N(\mathbf{0}, \sigma_e^2 Id)$  with  $N$  the Normal distribution of dimension  $N$ ,  $\mathbf{0}$  a vector of zeros, and  $Id$  the identity matrix of dimension  $N \times N$ . eBLUPs of  $\mathbf{g}$  were used instead of BLUEs as they are known to be more accurate for prediction and selection purposes, notably thanks to the shrinkage property (Piepho et al. 2008). Our goal was to test the null hypothesis  $\beta_p=0$  while controlling for relatedness between genotypes. Controlling the family-wise error rate at 5% to account for multiple testing, the effect of an SNP was deemed significant when the  $P$  value from the Wald test statistic was lower than the Bonferroni threshold.

The second type of models jointly analyzes all SNPs with the goal of selecting a subset of those with large effects while handling LD. This SNP selection can be achieved in a frequentist setting via stepwise regression (Segura et al. 2012). It starts with the SNP-by-SNP model, followed by inclusion, at every iteration, of the SNP with the smallest  $P$  value as an additional fixed effect, until the proportion of variance explained by the polygenic effect is close to zero. The SNP effects deemed significant were those of the best model selected according to the extended BIC. We fitted it with R/mlmm.gwas v1.0.4 (Bonnafous et al. 2018) allowing a maximum of 50 iterations. SNP selection can also be achieved in a Bayesian setting with the following model:  $eBLUP(\mathbf{g}) = \mathbf{1}\mu + M_a\boldsymbol{\beta} + \mathbf{e}$ , where  $M_a$  is a  $N \times P$  matrix of SNP genotypes (additive coding), with the so-called spike-and-slab prior for each SNP  $p$ ,  $\beta_p \sim \pi_0 \delta_0 + (1 - \pi_0) N_1(0, \sigma_\beta^2)$ ,  $\delta_0$  being a point mass at zero. We fitted it with the variational algorithm, faster than MCMC, implemented in R/varbvs version 2.5.7 (Carbonetto and Stephens 2012). An SNP was deemed significant when its posterior inclusion probability,  $PIP_p = \Pr(\beta_p \neq 0)$ , was higher than 0.80.

Beyond this focus on statistical significance (McShane and Gal 2017), we provide all estimates of significant additive SNP effects with a quantification of their uncertainty (Supplementary Table 5).

### QTL definition and annotation

QTLs were defined as intervals around significant SNPs based on LD decay (Bonnafous et al. 2018) (see Supplementary Text 3). A comparison was made between the QTLs detected in this study and (1) a first list of already-published QTLs (Vezzulli et al. 2019), significant at a 5% genome-wide threshold, that were classified according to the Vitis INRAE ontology v2 (<https://urgi.versailles.inra.fr/ephep/ephep>) and slightly edited for automatic processing (see Supplementary Text 3); and (2) a second list of significant hits from a few GWAS publications after converting their coordinates on the genome reference we used.

In terms of annotation, as a given locus can be a QTL for multiple response variables, we first merged our 489 reliable QTLs (found with at least 2 methods, see Results) across all response variables, which resulted in 134 distinct genomic intervals (Supplementary Table 9). These intervals had a median length of

100,001 kb (with a minimum of 100,001 kb and a maximum of 1,072,169 kb). We then searched for overlaps between them and the Vcost version 3 annotations totalizing 42,413 gene models from Canaguier et al. (2017), also using the correspondence between IGGP (International Grapevine Genome Program) and NCBI RefSeq gene model identifiers provided by the URGI (<https://urgi.versailles.inra.fr/Species/Vitis/Annotations>).

### Genetic architecture assumed dense

To estimate the proportion of variance of empirical BLUPs of genotypic values explained by the cumulative contribution of SNPs (Yang et al. 2010) (PVE<sub>SNPs</sub>), we used the well-known multi-SNP model termed ridge regression (also known as “RRBLUP”) which assumes a dense architecture:  $eBLUP(\mathbf{g}) = \mathbf{1}\mu + M_a\boldsymbol{\beta} + \mathbf{e}$  where  $\boldsymbol{\beta} \sim N_P(\mathbf{0}, \sigma_\beta^2 Id)$ . It is known to be equivalent to the “GBLUP” model (Habier et al. 2007; Vitezica et al. 2013):  $eBLUP(\mathbf{g}) = \mathbf{1}\mu + \mathbf{g}_a + \mathbf{e}$  where  $\mathbf{g}_a \sim N_N(\mathbf{0}, \sigma_a^2 A)$  with  $A$ , the  $N \times N$  matrix of additive genetic relationships, proportional to the matrix product  $M_a M_a^T$  once  $M_a$  is centered using allele frequencies. It is similar for the dominance genotypic values  $\mathbf{g}_d \sim N_N(\mathbf{0}, \sigma_d^2 D)$  where  $D$  is the  $N \times N$  matrix of dominance genetic relationships. Because the estimators of additive and dominance relationships from SNPs assume linkage equilibrium, a 0.5 LD threshold was applied when computing  $A$  and  $D$ . We fitted the models with R/lme4 and computed confidence intervals for variance components by bootstrap as above.

### Genomic prediction

Out-of-sample prediction was assessed within the panel by 5-fold cross-validation repeated 10 times with R/caret version 6 (Kuhn 2018), using R/varbvs that assumes a sparse genetic architecture and R/rrBLUP version 4.5 (Endelman 2011) that assumes a dense architecture (infinitesimal model). Note that the QTL results from the GWAS analysis were not used when training each model, to avoid overfitting. We assessed prediction accuracy between empirical BLUPs of genotypic values and their predictions with various metrics: root mean square error, Pearson’s linear correlation coefficient (corP), Spearman’s rank correlation coefficient (corS), as well as outputs from the simple linear regression of observations on predictions such as the intercept, slope, adjusted coefficient of determination ( $R^2$ ), and the  $P$ -value of the test for no bias.

Out-of-sample prediction was also assessed by training rrBLUP and varbvs methods on the whole panel and predicting empirical BLUPs of genotypic values for the 23 genotypes of the Syrah  $\times$  Grenache cross.

## Results

### Estimation of broad-sense heritability and genetic coefficient of variation

We took advantage of the *V. vinifera* L. panel of 279 cultivars suitable for GWAS and representing the INRAE Vassal germplasm repository to set up a randomized-complete-block field trial (Supplementary Fig. 1). It was phenotyped for 127 traits from which 25 extra variables were computed. All 152 response variables displayed substantial variation (Supplementary Fig. 5). For some polyphenol variables, part of the variation was obviously associated with skin color, 137 cultivars out of 279 having colored skin berries. When phenotyped, the control cultivar allowed us to establish that (1) part of this variation was due to genetic differences between panel cultivars (Supplementary Fig. 5), and that (2) spatial heterogeneity was negligible (Supplementary Fig. 6).

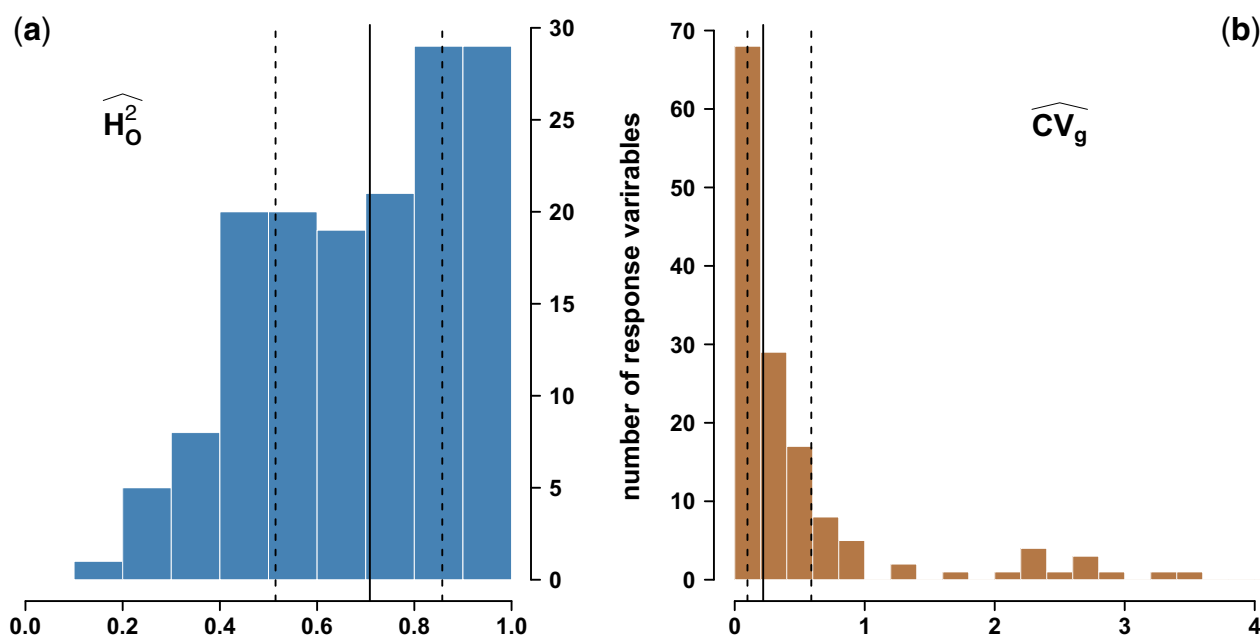


**Fig. 1.** Estimation in a diverse panel of *Vitis vinifera* L. of (a) broad-sense heritabilities for 152 response variables using the estimator from Oakey et al. (2006),  $H_o^2$ , and (b) their genetic coefficients of variation,  $CV_g$ . Vertical lines indicate the median (plain), and quantiles at 0.25 and 0.75 (dotted).

The amount of missing data among response variables ranged from 15.78% to 43.93% (Supplementary Table 4). To account for such unbalance, we fitted linear mixed models and obtained BLUPs of genotypic values. After model selection, the final set of fixed and random effects differed between response variables (Supplementary Table 4), with year and genotype–year interaction effects being selected in most cases.

We then assessed the accuracy with which genotypic values were estimated using broad-sense heritability (the higher, the better). As shown in Fig. 1, 76.6% of broad-sense heritability estimates were above 0.5, with narrow confidence intervals (Supplementary Table 4). Two estimators,  $H_C^2$  and  $H_o^2$ , handling missing data differently, gave very similar estimates (Supplementary Table 4), thus indicating that genotypic values of all cultivars were accurately estimated for most response variables. Moreover, 92.7% of the genetic coefficients of variation were above 5% and 59.1% above 20% (Fig. 1; Supplementary Table 4).

### Combining genotyping technologies to explain more genetic variance

We then aimed to explain the variance of these genotypic BLUPs with SNP genotypes. For that purpose, we used 2 sets of SNPs, the “microarray-only SNPs” (10,503 SNPs) and “microarray-GBS SNPs” (63,105 SNPs).

Because LD is known to be short in *V. vinifera* L. (Myles et al. 2011; Nicolas et al. 2016), we increased the SNP density initially obtained with the microarray by sequencing with complexity reduction (GBS). Raw reads had high quality along their sequences, although many displayed adapters’ content at their 5’ end, which had to be trimmed off. After demultiplexing, more than 95% of the reads were assigned to a cultivar. After alignment on the reference genome, the median coverage depth of regions having at least 1 read, averaged over cultivars, was 21.7, which allowed to accurately call both homozygous and heterozygous SNP genotypes after filtering out SNPs supported by <10 reads.

Compared with the microarray-only SNP set, the combined microarray-GBS set displayed a substantially higher SNP density

along all chromosomes (Supplementary Fig. 4). We then estimated the additive genetic relationships between cultivars (Supplementary Fig. 7), confirming the weak structure in 3 sub-groups corresponding to wine west, wine east, and table east. The matrix of genetic relationships was used to estimate the proportion of variance in genotypic BLUPs explained by SNPs ( $PVE_{SNPs}$ ). Assuming an additive-only, polygenic architecture,  $PVE_{SNPs}$  was higher with microarray-GBS SNPs than with microarray-only SNPs for 97.8% of responses variables (Fig. 2; Supplementary Table 5). This showed the advantage of combining SNPs so that more QTLs are in LD with at least 1 genotyped SNP.

Models with both additive and dominance relationships either failed to converge or then, only with difficulty, most probably because the matrix of dominance relationships was very similar to the identity matrix, making it indistinguishable from the error term (Supplementary Fig. 7).

### QTL detection by GWAS and identification of candidate genes

The GWAS methods used in the following were first checked on 2 previously phenotyped traits, flower sex and berry skin color, for which the already known genetic architecture consists in a major QTL. Results were coherent with the literature (Fournier-Level et al. 2009; Picq et al. 2014): a major QTL on chromosome 2 for flower sex (around coordinate 4,769,151) and for berry skin color (around coordinate 15,753,009). Other weaker QTLs were also found, on the Unknown chromosome for flower sex [note that Tello et al. (2019) found chunks of chromosome 2 in the Unknown chromosome when building genetic maps], and on chromosome 7 and 13 for berry skin color (consistent with QTLs for skin anthocyanidin content found by Guo et al. 2015).

Each response variable phenotyped in this study was analyzed with an SNP-by-SNP model to identify significant SNPs (Supplementary Table 6). For each response variable, QTLs were defined as LD-based intervals around each significant SNP (Supplementary Table 7), and then merged when overlapping (Supplementary Table 8). As summarized in Table 1, at least 1

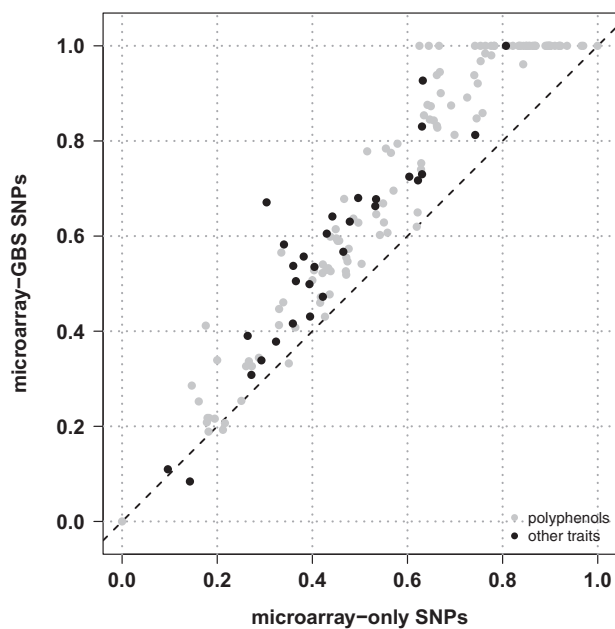


**Fig. 2.** Estimation in a diverse panel of *Vitis vinifera* L. of the proportion of variance in genotypic BLUPs explained by SNPs for 152 response variables and 2 SNP densities, assuming an additive-only, polygenic architecture.

**Table 1.** Comparison between methods in terms of the number of QTLs (#QTLs) found in a diverse panel of *Vitis vinifera* L. for 2 SNP data sets, summed up over all response variables.

Method		Microarray-only SNPs			Microarray-GBS SNPs		
Model	Software	#RVs	#sSNPs	#QTLs	#RVs	#sSNPs	#QTLs
SNP-by-SNP	GEMMA	88	2,295	1,179	101	7,855	1,784
Multi-SNP	mlmm.gwas	148	1,257	1,243	125	703	692
	Varbvs	118	266	257	119	258	257

Also indicated are the number of response variables with at least one QTL (#RVs), and the number of significant SNPs (#sSNPs).

QTL was found for 66.4% of response variables with the microarray-GBS SNPs, when compared with 57.9% with the microarray-only SNPs.

To benefit from a potential gain in power, we fitted 2 multi-SNP models that both provided more response variables with at least 1 QTL compared with the SNP-by-SNP model, whatever the SNP set (Table 1). Within multi-SNP methods, mlmm.gwas found more significant SNPs and QTLs than varbvs, and for more response variables. Yet, the interpretation is not straightforward as these methods do not use the same criterion for declaring an SNP as significant. Surprisingly, for mlmm.gwas, the numbers of response variables with at least 1 QTL, significant SNPs and QTLs were lower with more tested SNPs.

By summing over the 150 response variables with at least 1 QTL, a total of 3,490 QTLs were found (Supplementary Table 8), which corresponded to an increase of 196% in the number of QTLs and of 70% in the number of response variables with at least 1 QTL, compared with applying the SNP-by-SNP method on the microarray-only SNPs. Among these QTLs, 136 were found by all 3 methods, while 3,001 were found by a single method only and 1,598 by multi-SNP methods only (Supplementary Fig. 9). Furthermore, over these 150 response variables, 26 had no QTL according to the SNP-by-SNP method but at least one found by both multi-SNP methods (Supplementary Fig. 10).

All chromosomes harbored at least 1 QTL (Supplementary Fig. 11), and most QTLs found only by the multi-SNP mlmm.gwas method fell far from QTLs found by other methods (Supplementary Fig. 12). Moreover, 90% of the QTLs found only by the SNP-by-SNP method GEMMA clustered on chromosome 2 for 64 response variables, all of them being polyphenols, in relation with the anthocyanin-related MYB genes on this chromosome (Matus et al. 2008). This was expected because GEMMA ignores LD between SNPs. In contrast, the multi-SNP varbvs method was more parsimonious, yet had enough power to identify significant SNPs in regions in which GEMMA did not identify any signal (Supplementary Fig. 12).

To prioritize QTLs for further investigation, 489 QTLs involving 124 response variables were deemed reliable as they were found by at least 2 methods (Supplementary Table 9 and Supplementary Fig. 13). They corresponded to 59% less QTLs but 41% more response variables with at least 1 QTL, compared with applying the SNP-by-SNP method on the microarray-only SNPs. All chromosomes harbored at least 1 such reliable QTL, except chromosome 19 (Fig. 3).

The 489 reliable QTLs were compared with the largest list of QTLs detected in grapevine bi-parental crosses compiled so far (Vezzulli et al. 2019). Among the 22 traits in common, QTLs were found on the same chromosome for 7 only (Supplementary Table 8): cluster number (on chromosome 7), berry weight (on chromosomes 1, 2, 8, 11, 15, and 17), malate (on chromosomes 9 and 18), glucose to fructose ratio (on chromosome 2), mean degree of polymerization of tannins (chromosome 17), total concentration of native anthocyanins (on chromosome 2), and %B-ring methylated anthocyanins (on chromosome 2).

We also compared our reliable QTLs with significant GWAS hits published in grapevine. Only 2 traits (cluster and berry weight) were phenotyped in at least 1 other study with at least 1 significant GWAS hit found (Zarouri 2016; Laucou et al. 2018; Guo et al. 2019). For berry weight, out of the 10 QTLs we found, 8 were deemed new on chromosomes 1, 2, 8, 11, 15, and 17. We also found 2 QTLs on chromosome 8 close to a known GWAS hit (Zarouri 2016), but did not recover other hits on chromosomes 5, 17, 18, and 19 as in Zarouri (2016) and Guo et al. (2019). For cluster weight, we found 2 new QTLs on chromosomes 1 and 3 but did not recover other hits on chromosomes 5 and 13 (Zarouri 2016; Laucou et al. 2018).

The comparison of our reliable QTLs with the reference gene annotations detected 1,926 distinct gene models (Supplementary Table 10). Out of these, only 980 had a proposed putative function (Supplementary Table 11).

## Assessment of genomic prediction and insight into genetic architectures

We assessed the accuracy of genomic prediction by cross-validation within the panel of 279 cultivars (Supplementary Table 12). We compared 2 methods assuming contrasted genetic architectures: additive infinitesimal for rrBLUP and additive sparse for varbvs. Both the median Pearson and Spearman correlation coefficients between observed and predicted genotypic values fell between 0.37 and 0.44, similarly for both SNP sets and methods (Fig. 4). These correlations showed substantial correlation with broad-sense heritability (Supplementary Fig. 14), higher for varbvs (~0.65) than for rrBLUP (~0.54). However, the distributions of varbvs' correlation coefficients were clearly multi-modal, with the majority being lower than rrBLUP's but still a substantial fraction being higher. This confirmed the robustness of rrBLUP's predictions irrespective of the underlying architecture (Wang et al. 2015). Yet varbvs can provide substantially better predictions than

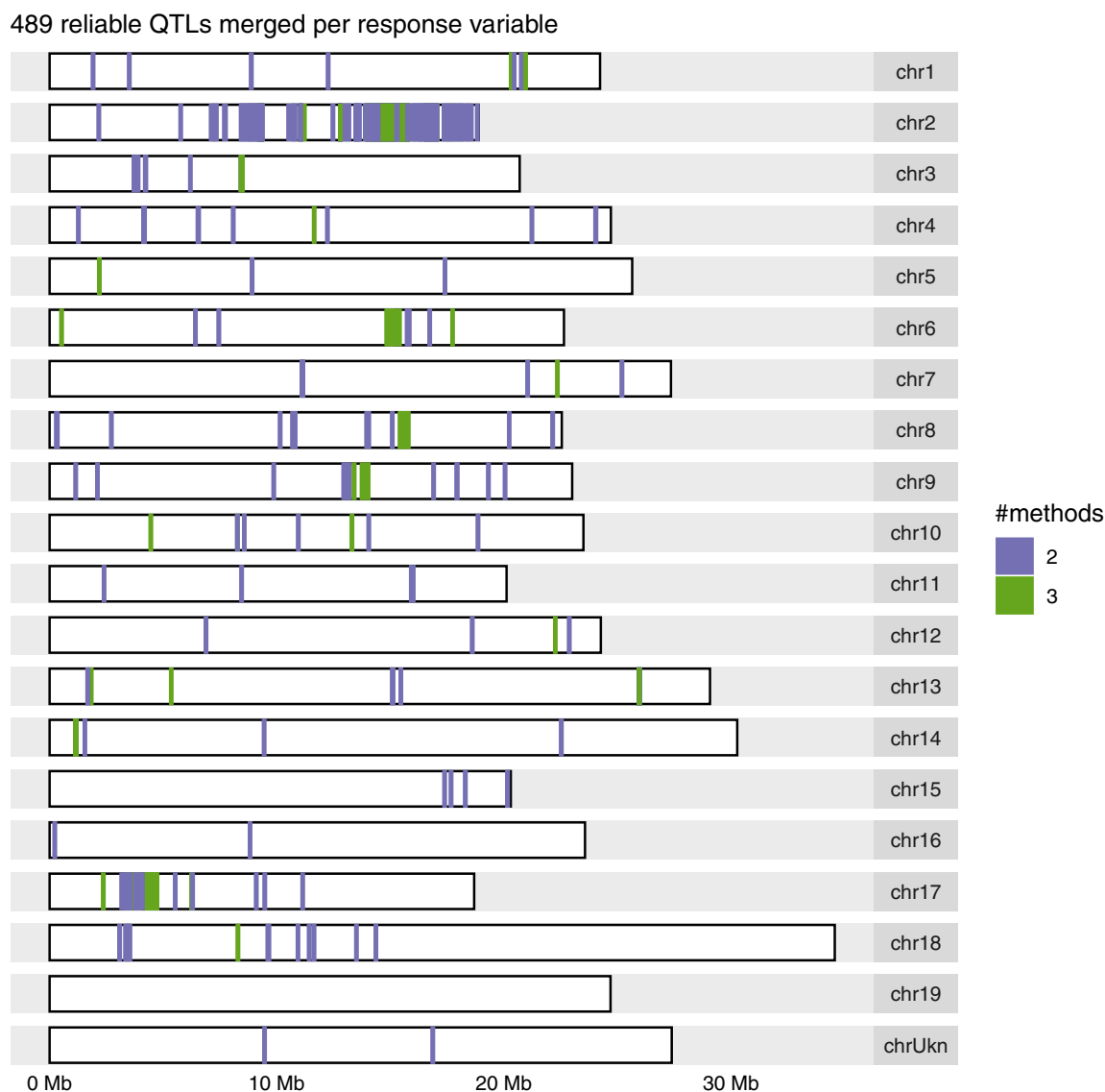


**Fig. 3.** Genomic distribution of the most reliable QTLs identified by 2 methods in a diversity panel of *Vitis vinifera* L. after merging them over microarray-only and microarray+GBS SNP sets per response variable. The color legend indicates the number of methods that identified a given QTL.

rrBLUP for traits for which the genetic architecture is likely to be rather sparse.

Moreover, rrBLUP results did not seem to depend on the SNP set whereas they were slightly better with the microarray-GBS SNPs for varbvs. This suggests that, among the extra SNPs provided by GBS, varbvs managed to identify those that improved its prediction accuracy. Concerning the  $P$  value of the test for no bias, varbvs showed similar values across both SNP sets, higher than rrBLUP in general and above 0.05, suggesting an absence of bias. On the contrary, rrBLUP showed lower  $P$  values with the microarray-GBS SNPs, suggesting that its assumption of all SNP effects being nonzero may be too strong for these traits, especially when SNP density is high.

We also used the 279 cultivars panel as a training set to predict MBW in a subset of a Syrah  $\times$  Grenache progeny. With rrBLUP (respectively, varbvs), this gave a Pearson correlation of 0.56 (0.35), an adjusted coefficient of regression of 0.28 (0.08), and a  $P$  value of  $1.6 \times 10^{-4}$  ( $3.5 \times 10^{-3}$ ) when testing for no bias.

The correlation is particularly promising for rrBLUP compared with varbvs, in agreement with the results obtained by cross-validation within the panel (Pearson correlation of 0.71 with rrBLUP and 0.61 with varbvs).

Finally, combining results from both genome-wide association and genomic prediction studies provides insight into the genetic architecture of the studied traits. In Table 2, trait classes are sorted according to the following metric: the difference between the accuracy of genomic prediction assuming a sparse additive genetic architecture (as implemented in varbvs) vs a dense one (as implemented in rrBLUP), using the Spearman correlation coefficient from the cross-validation above as a proxy of prediction accuracy (Supplementary Table 13).

Overall, the median of this metric is positive only for response variables corresponding to biochemical traits (mostly polyphenols), suggesting they display a sparse genetic architecture. All other trait classes have a negative median metric, suggesting a dense genetic architecture. When taking into account the

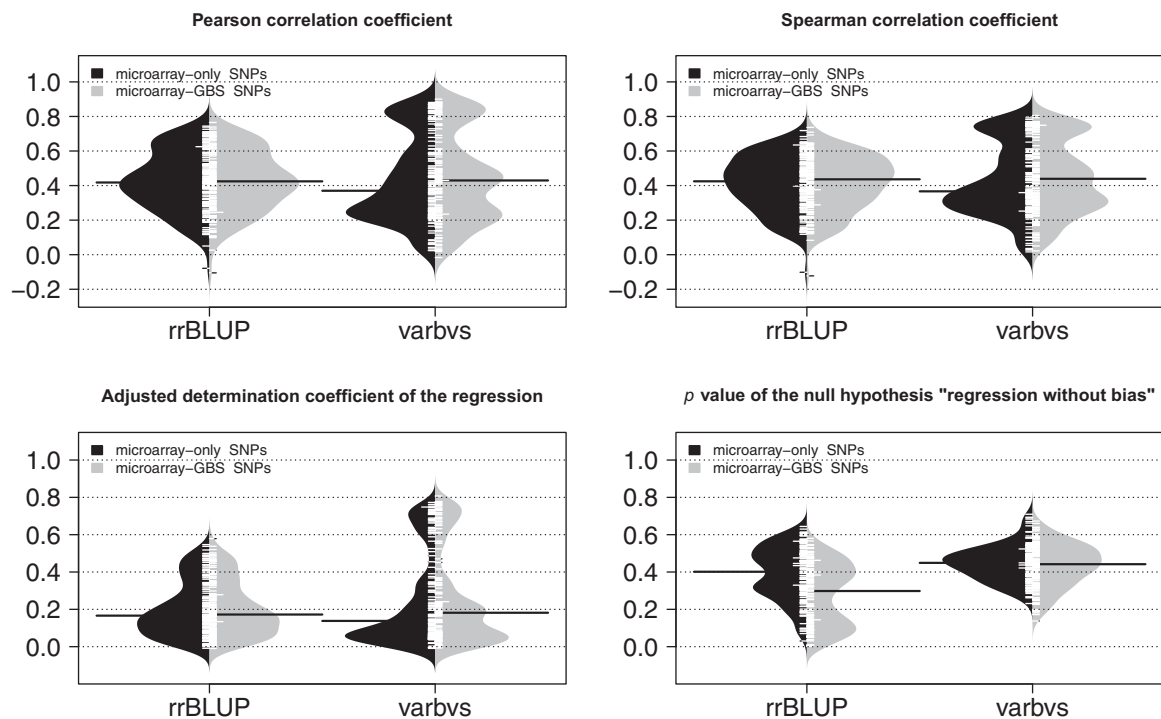


**Fig. 4.** Assessment of genomic prediction accuracy within a diversity panel of *Vitis vinifera* L. by repeated 5-fold cross-validations, comparing 2 SNP sets (microarray-only and microarray-GBS) and 2 methods (rrBLUP assuming a dense genetic architecture and varbvs assuming a sparse genetic architecture) for 152 response variables. The 4 displayed metrics were averaged over folds and replicates.

**Table 2** Types of additive genetic architecture per trait class in a diversity panel of *Vitis vinifera* L. based on the accuracy of genomic prediction assuming a sparse genetic architecture (method “varbvs”) or a dense one (method “rrBLUP”) over all response variables (RVs).

Trait class	#RVs	Median of $\text{cor}_S(\text{varbvs}) - \text{cor}_S(\text{rrBLUP})$	Additive genetic architecture	#relQTLs	$H_0^2$
Biochemical	136	+0.05 [−0.12, +0.18]	Sparse (−)	3.0 [0.0, 8.0]	0.69 [0.41, 0.96]
Abiotic stress	2	−0.04 [−0.09, +0.02]	Dense (−)	0.5 [0.1, 0.9]	0.37 [0.21, 0.52]
Phenological	3	−0.04 [−0.06, −0.03]	Dense (+)	2.0 [0.4, 2.0]	0.80 [0.72, 0.83]
Morphological	5	−0.08 [−0.08, −0.07]	Dense (+)	1.0 [0.0, 1.6]	0.82 [0.74, 0.87]
Agronomical	6	−0.12 [−0.09, +0.19]	Dense (−)	1.5 [0.5, 5.0]	0.79 [0.38, 0.95]

Also indicated are a symbol for the confidence level in the classification (+ for high, − for low), the number of reliable QTL (#relQTLs) and the broad-sense heritability estimated according to [Oakey et al. \(2006\)](#) ( $H_0^2$ ); for both, the median, quantile at 10% and quantile at 90 are given.

distribution of the metric, the classification in sparse or dense architecture is deemed more trustworthy when the quantile interval does not include 0, which is the case for phenological and morphological traits.

Apart from the abiotic stress variable  $\delta^{13}\text{C}$ , all response variables had a high median broad-sense heritability (around 0.7 and above), indicating a higher measurement quality, hence also contributing to increased trustworthiness in the suggested genetic architecture. Moreover, in the case of the biochemical response variables, the median number of reliable QTLs is higher than for the other trait classes, although there is a large variation. This is consistent with their genetic architecture deemed sparse, for which one expects to have QTLs with an effect large-enough to be found significant.

## Discussion

### Design and analysis of field trials for perennials

Acquiring phenotypic data from which genotypic values can be deduced with sufficient accuracy is a major challenge, especially because a large panel is a prerequisite to provide enough statistical power to detect QTLs ([Nicolas et al. 2016](#)). Our randomized

block design certainly helped in reaching medium to high broad-sense heritability for most traits. Those with low heritability may be linked to the difficulty of sampling fruits at a similar physiological stage, a particularly pressing issue for grapevine due to the strong intra- and inter-cluster heterogeneity between berries ([Shahood 2017](#)). Automating new protocols ([Bigard et al. 2018](#)) remains to be done to phenotype large panels.

At the first stage of the analysis, we chose to include PRUW, the number of wooding shoots and vigor as explanatory factors in the global model, but neither flower sex nor berry color. Our rationale was that the former 3 are more influenced by the way the field trial is conducted than the latter 2, which are under a stronger genetic determinism ([Fournier-Level et al. 2009](#); [Picq et al. 2014](#)). This approach would hence keep most genetically based variation between genotypes for the second stage of the analysis (genome-wide association and genomic prediction). More generally, this raises the question of how to deal with multiple traits to exploit their correlations (Supplementary Table 14 and Supplementary Fig. 15). Most multivariate linear models place all the traits on the same level, which complicates the understanding of their genetic architecture ([Kemper et al. 2018](#)). A more ambitious approach would leverage functional-structural plant









- Oakey H, Verbyla A, Pitchford W, Cullis B, Kuchel H. Joint modeling of additive and non-additive genetic line effects in single field trials. *Theor Appl Genet.* 2006;113(5):809–819. doi:10.1007/s00122-006-0333-z.
- Ollé D, Guiraud JL, Souquet JM, Terrier N, Ageorges A, Cheynier V, Verries C. Effect of pre- and post-veraison water deficit on proanthocyanidin and anthocyanin accumulation during Shiraz berry development: water stress and flavonoid biosynthesis. *Aust J Grape Wine Res.* 2011;17(1):90–100. doi:10.1111/j.1755-0238.2010.00121.x.
- Pebesma EJ. Multivariable geostatistics in S: the gstat package. *Comput Geosci.* 2004;30(7):683–691. doi:10.1016/j.cageo.2004.03.012.
- Phukan UJ, Jeena GS, Shukla RK. WRKY transcription factors: molecular regulation and stress responses in plants. *Front Plant Sci.* 2016;7(760):1–14. doi:10.3389/fpls.2016.00760. <http://journal.frontiersin.org/Article/10.3389/fpls.2016.00760/abstract> [accessed 2021 Jan 5].
- Picq S, Santoni S, Lacombe T, Latreille M, Weber A, Ardisson M, Ivorra S, Maghradze D, Arroyo-Garcia R, Chatelet P, et al. A small XY chromosomal region explains sex determination in wild dioecious *V. vinifera* and the reversal to hermaphroditism in domesticated grapevines. *BMC Plant Biol.* 2014;14:229. doi:10.1186/s12870-014-0229-z.
- Piepho HP, Möhring J, Melchinger AE, Büchse A. BLUP for phenotypic selection in plant breeding and variety testing. *Euphytica.* 2008; 161(1–2):209–228. doi:10.1007/s10681-007-9449-8.
- Pinasseau L, Vallverdú-Queralt A, Verbaere A, Roques M, Meudec E, Le Cunff L, Péros J-P, Ageorges A, Sommerer N, Boulet J-C, et al. Cultivar diversity of grape skin polyphenol composition and changes in response to drought investigated by LC-MS based metabolomics. *Front Plant Sci.* 2017;8:1826. doi:10.3389/fpls.2017.01826.
- Pinasseau L, Verbaere A, Roques M, Meudec E, Vallverdu-Queralt A, Ollier L, Marlin T, Guiraud J-L, Berger G, Bertrand Y, et al. Innovine WP3: 105 phenolic compound quantification of 2014 and 2015 mature grape berries from a core-collection of 279 irrigated and non-irrigated *Vitis vinifera* cultivars; 2017. doi:10.5281/ZENODO.574857. [accessed 2020 Aug 27]. <https://zenodo.org/record/574857>
- Rex F, Fechter I, Hausmann L, Töpfer R. QTL mapping of black rot (*Guignardia bidwellii*) resistance in the grapevine rootstock 'Börner' (*V. riparia* Gm183 × *V. cinerea* Arnold). *Theor Appl Genet.* 2014;127(7):1667–1677. doi:10.1007/s00122-014-2329-4.
- Rienth M, Torregrosa L, Sarah G, Ardisson M, Brillouet J-M, Romieu C. Temperature desynchronizes sugar and organic acid metabolism in ripening grapevine fruits and remodels their transcriptome. *BMC Plant Biol.* 2016;16(164):1–23. doi:10.1186/s12870-016-0850-0.
- Rinaldo A, Cavallini E, Jia Y, Moss SMA, McDavid DAJ, Hooper LC, Robinson SP, Tornielli GB, Zenoni S, Ford CM, et al. A grapevine anthocyanin acyltransferase, transcriptionally regulated by VvMYBA, can produce most acylated anthocyanins present in grape skins. *Plant Physiol.* 2015;169:1897–1916. doi:10.1104/pp.15.01255.
- Roth M, Muranty H, Di Guardo M, Guerra W, Patocchi A, Costa F. Genomic prediction of fruit texture and training population optimization towards the application of genomic selection in apple. *Hortic Res.* 2020;7(1):148. doi:10.1038/s41438-020-00370-5.
- Sargolzaei M, Maddalena G, Bitsadze N, Maghradze D, Bianco PA, Failla O, Toffolatti SL, De Lorenzis G. Rpv29, Rpv30 and Rpv31: three novel genomic loci associated with resistance to *Plasmopara viticola* in *Vitis vinifera*. *Front Plant Sci.* 2020;11:562432. doi:10.3389/fpls.2020.562432.
- Savchenko TV, Rolletschek H, Dehesh K. Jasmonates-mediated rewiring of central metabolism regulates adaptive responses. *Plant Cell Physiol.* 2019;60(12):2613–2620. doi:10.1093/pcp/pcz181.
- Schweiger R, Kaufman S, Laaksonen R, Kleber ME, März W, Eskin E, Rosset S, Halperin E. Fast and accurate construction of confidence intervals for heritability. *Am J Hum Genet.* 2016;98(6): 1181–1192. doi:10.1016/j.ajhg.2016.04.016.
- Segura V, Vilhjalmsón B, Platt A, Korte A, Seren U, Long Q, Nordborg M. An efficient multi-locus mixed-model approach for genome-wide association studies in structured populations. *Nat Genet.* 2012;44(7):825–830. doi:10.1038/ng.2314.
- Segurel MA, Razungles AJ, Riou C, Trigueiro MGL, Baumes RL. Ability of possible DMS precursors to release DMS during wine aging and in the conditions of heat-alkaline treatment. *J Agric Food Chem.* 2005;53(7):2637–2645. doi:10.1021/jf048273r.
- Shahood R. La baie au sein d'une vendange asynchrone: Un nouveau paradigme vers l'interprétation quantitative des flux de sucres et acides en tant qu'osmotocums et substrat respiratoires majeurs lors du développement bimodal du raisin [PhD]. [Montpellier, France]: Montpellier SupAgro; 2017. <https://www.theses.fr/s206075>.
- Sievanen R, Godin C, DeJong TM, Nikinmaa E. Functional-structural plant models: a growing paradigm for plant studies. *Ann Bot.* 2014;114(4):599–603. doi:10.1093/aob/mcu175.
- Simpson JP, Di Leo R, Dhanoa PK, Allan WL, Makhmoudova A, Clark SM, Hoover GJ, Mullen RT, Shelp BJ. Identification and characterization of a plastid-localized Arabidopsis glyoxylate reductase isoform: comparison with a cytosolic isoform and implications for cellular redox homeostasis and aldehyde detoxification. *J Exp Bot.* 2008;59(9):2545–2554. doi:10.1093/jxb/ern123.
- Sun L, Li S, Jiang J, Tang X, Fan X, Zhang Y, Liu J, Liu C. New quantitative trait locus (QTLs) and candidate genes associated with the grape berry color trait identified based on a high-density genetic map. *BMC Plant Biol.* 2020;20(1):302. doi:10.1186/s12870-020-02517-x.
- Swarts K, Li H, Romero Navarro JA, An D, Romay MC, Hearne S, Acharya C, Glaubitz JC, Mitchell S, Elshire RJ, et al. Novel methods to optimize genotypic imputation for low-coverage, next-generation sequence data in crop plants. *Plant Genome.* 2014;7(3):1–12. doi:10.3835/plantgenome2014.05.0023.
- Tello J, Roux C, Chouiki H, Laucou V, Sarah G, Weber A, Santoni S, Flutre T, Pons T, This P, et al. A novel high-density grapevine (*Vitis vinifera* L.) integrated linkage map using GBS in a half-diallel population. *Theor Appl Genet.* 2019;132(8):2237–2252. doi:10.1007/s00122-019-03351-y.
- Terrier N, Sauvage F-X, Ageorges A, Romieu C. Changes in acidity and in proton transport at the tonoplast of grape berries during development. *Planta.* 2001;213(1):20–28. doi:10.1007/s004250000472.
- Vezzulli S, Doligez A, Bellin D. Molecular mapping of grapevine genes. In: D Cantu, MA Walker, editors. *The Grape Genome (Compendium of Plant Genomes)*. Cham: Springer International Publishing; 2019. p. 103–136. [http://link.springer.com/10.1007/978-3-030-18601-2\\_7](http://link.springer.com/10.1007/978-3-030-18601-2_7) [accessed 2021 Feb 4].
- Vezzulli S, Zulini L, Stefanini M. Genetics-assisted breeding for downy/powdery mildew and phylloxera resistance at fem. *BIO Web Conf.* 2019;12:01020. doi:10.1051/bioconf/20191201020.
- Vitezica Z, Varona L, Legarra A. On the additive and dominant variance and covariance of individuals within the genomic selection scope. *Genetics.* 2013;195(4):1223–1230. doi:10.1534/genetics.113.155176.
- Wang M, Vannozzi A, Wang G, Liang Y-H, Tornielli GB, Zenoni S, Cavallini E, Pezzotti M, Cheng Z-M. Genome and transcriptome analysis of the grapevine (*Vitis vinifera* L.) WRKY gene family. *Hortic Res.* 2014;1(1):14016. doi:10.1038/hortres.2014.16.
- Wang X, Yang Z, Xu C. A comparison of genomic selection methods for breeding value prediction. *Sci Bull.* 2015;60(10):925–935. doi:10.1007/s11434-015-0791-2.

- Wimmer V, Lehermeier C, Albrecht T, Auinger H-J, Wang Y, Schon C-C. Genome-wide prediction of traits with different genetic architecture through efficient variable selection. *Genetics*. 2013;195(2): 573–587. doi:10.1534/genetics.113.150078.
- Wolkovich EM, García de Cortázar-Atauri I, Morales-Castilla I, Nicholas KA, Lacombe T. From Pinot to Xinomavro in the world's future wine-growing regions. *Nature Clim Change*. 2018;8(1): 29–37. doi:10.1038/s41558-017-0016-6.
- Xie X, Huang A, Gu W, Zang Z, Pan G, Gao S, He L, Zhang B, Niu J, Lin A, et al. Photorespiration participates in the assimilation of acetate in *Chlorella sorokiniana* under high light. *New Phytol*. 2016; 209(3):987–998. doi:10.1111/nph.13659.
- Xu S. Theoretical basis of the Beavis effect. *Genetics*. 2003;165(4): 2259–2268.
- Yang J, Benyamin B, McEvoy B, Gordon S, Henders A, Nyholt D, Madden P, Heath A, Martin N, Montgomery G, et al. Common SNPs explain a large proportion of the heritability for human height. *Nat Genet*. 2010;42(7):565–569. doi:10.1038/ng.608.
- Yang X, Guo Y, Zhu J, Niu Z, Shi G, Liu Z, Li K, Guo X. Genetic diversity and association study of aromatics in grapevine. *J Amer Soc Hort Sci*. 2017;142(3):225–231. doi:10.21273/JASHS04086-17.
- Yu B, Lin Z, Li H, Li X, Li J, Wang Y, Zhang X, Zhu Z, Zhai W, Wang X, et al. TAC1, a major quantitative trait locus controlling tiller angle in rice. *Plant J*. 2007;52(5):891–898. doi:10.1111/j.1365-3113X.2007.03284.x.
- Yu K, Jun JH, Duan C, Dixon RA. VvLAR1 and VvLAR2 are bifunctional enzymes for proanthocyanidin biosynthesis in grapevine. *Plant Physiol*. 2019;180(3):1362–1374. doi:10.1104/pp.19.00447.
- Zarei A, Brikis CJ, Bajwa VS, Chiu GZ, Simpson JP, DeEll JR, Bozzo GG, Shelp BJ. Plant glyoxylate/succinic semialdehyde reductases: comparative biochemical properties, function during chilling stress, and subcellular localization. *Front Plant Sci*. 2017;8: 1399. doi:10.3389/fpls.2017.01399.
- Zarouri B. Association study of phenology, yield and quality related traits in table grapes using SSR and SNP markers. Universidad Politécnica de Madrid, 2016. [http://oa.upm.es/43315/1/BELKACEM\\_ZAROURI.pdf](http://oa.upm.es/43315/1/BELKACEM_ZAROURI.pdf).
- Zhang H, Fan X, Zhang Y, Jiang J, Liu C. Identification of favorable SNP alleles and candidate genes for seedlessness in *Vitis vinifera* L. using genome-wide association mapping. *Euphytica*. 2017; 213(7):1–13. doi:10.1007/s10681-017-1919-z. <http://link.springer.com/10.1007/s10681-017-1919-z> [accessed 2018 Mar 9].
- Zhang Y-M, Jia Z, Dunwell JM. Editorial: the applications of new multi-locus GWAS methodologies in the genetic dissection of complex traits. *Front Plant Sci*. 2019;10:100. doi:10.3389/fpls.2019.00100.
- Zhou X, Stephens M. Genome-wide efficient mixed-model analysis for association studies. *Nat Genet*. 2012;44(7):821–824. doi: 10.1038/ng.2310.

Communicating editor: A. Paterson